TITLE NO. 74-28

Investigation of Reinforced Concrete Walls

By GAROLD D. OBERLENDER and NOEL J. EVERARD

Fifty-four precast concrete walls were tested to failure in order to obtain test data for comparison with analytical methods for wall design prescribed by the ACI Building Code (ACI 318-71). The empirical method of Chapter 14 and the method of designing walls as columns under Chapter 10 of the ACI Building Code are both investigated.

Keywords: axial loads; **bearing walls**; columns (supports); compressive strength; **failure**; loads (forces); **precast concrete**; reinforced concrete; slenderness ratio; **structural analysis**; structural design; **ultimate strength method**; **walls.**

■ AN EXPERIMENTAL RESEARCH INVESTIGATION of precast reinforced concrete load-bearing walls was initiated in the summer of 1971 and completed the early part of 1973 at The University of Texas at Arlington. The investigation has provided a great deal of experimental information concerning the ultimate strength and structural behavior of reinforced concrete load-bearing wall panels.

This was accomplished by testing to failure a series of 54 wall panels. Walls with cross-sectional dimensions 3 in. (7.62 cm) thick and 24 in. (60.96 cm) wide were constructed with heights varying from 2 to 7 ft (60.96 to 213.36 cm), in increments of 1 ft (30.48 cm). Various quantities and locations of reinforcements were used in the testing program. In addition, two different load conditions, concentric load and loads at the edge of the kern region, were applied to specimens for each wall configuration. Each wall was tested to destruction. Deflections and strains were measured for all load increments.

ACI member **Garold D. Oberlender** is associate professor and head of construction management technology, School of Engineering Technology, Oklahoma State University, Stillwater, Okla.

Noel J. Everard, FACI, is professor and chairman of civil engineering at the University of Texas at Arlington, Tex. He is a member of ACI Committees 224, Cracking, 318, Standard Building Code, 340, Strength Design Handbook, and 443, Concrete Bridge Design. He is a former member of the Technical Activities Committee.

A 3 in. (7.62 cm) thickness was chosen as a half-scale model, considering the required minimum 6 in. (15.24 cm) thickness for wall design by Chapter 14 of "Building Code Requirements for Reinforced Concrete (ACI 318-71)."[1] The wall heights of 2 through 7 ft (60.96 to 213.36 cm) were then selected to provide a range of height-to-thickness ratios from 8 to 28. The ratio 28 slightly exceeds the maximum value of 25 permitted by Chapter 14 of the ACI Building Code for wall design, but falls within the scope of Chapter 10 of the code, which does not limit ratio of height to thickness.

Two sizes of reinforcement were used in the investigation: 4 x 4–6 x 6 and 4 x 4–8 x 8 smooth round welded wire fabric, conforming to ASTM A 185 specifications. Reinforcement was placed symmetrically in the panels in two separate layers with a cover of 5/8 in. (1.5875 cm). This provided a ratio of area of steel to gross area of concrete A_s/A_g of 0.0047 for the #6 gage (approx. 0.5 cm) wire and 0.0033 for the #8 gage (approx. 0.4 cm) wire specimens. These values are above the minimum ratios required by Chapter 14 of the ACI Building Code, and were selected to obtain test results in the usual ranges of reinforcement used in wall design.

In an effort to determine the effect of location of the reinforcement, six walls were cast with a 3/8 in. (0.9525 cm) cover instead of 5/8 in. (1.5875 cm) cover on the steel reinforcement. Two walls of each wall height of 3, 5, and 7 ft (91.44, 152.4, and 213.36 cm) were constructed with #8 gage reinforcement. This selection provided for two loading conditions, eccentric and concentric, for each wall height cast with the minimum cover of 3/8 in. (0.9525 cm). Fig. 1 presents a cross section of the three geometric configurations for reinforcement used in the test program.

The intent of the test program was to determine the strength of reinforced concrete load-bearing wall panels with respect to geometric configuration. Strength of concrete was varied between 4000 psi and 6000 psi which corresponded to the usual range of concrete strength used in wall design. Standard 6 in. (15.24 cm) diameter test cylinders

were obtained from the mix for each wall. The concrete strength of these cylinders was used in the analysis of failure loads in dimensionless quantities. Table 1 is a summary of cylinder strengths. Tensile tests were conducted on 6 random samples of each of the #6 and #8 gage wire reinforcements. For the measured diameters of each type of reinforcement, the tensile strength varied from 73 ksi (5128.25 kgf/cm^2) to 86 ksi (6041.50 kgf/cm^2). A complete presentation of concrete and reinforcement strength is provided in Reference 2.

All walls in the experimental program were tested with a uniformly distributed axial load along their ends. One-half of the walls were tested with the load located concentrically along the centroidal axis of the cross section, and one-half of the walls were tested with the load located eccentrically ½ in. (1.27 cm) off the centroidal axis in the transverse direction. The ½ in. (1.27 cm) eccentricity provided an e/h value of 1/6, which is the outermost position of the load permitted for wall design by Chapter 14 of the ACI Building Code. Loads were not applied in the lateral or transverse directions of any wall panel in this experimental program. Table 2 is a summary of load conditions for each panel tested in the investigation.

The results of ultimate loads of the model walls in the experimental program were obtained as dimensionless quantities to allow comparisons with several analytical methods of analysis. Interaction curves were developed for each wall configuration in the test program and used to predict the strength of the model walls in accordance with Chapter 10 of the ACI Building Code. The test results of ultimate loads of the model walls were also compared with the empirical design method for walls contained in Chapter 14 of the ACI Building Code.

The structural behavior of the walls was observed by measuring surface strains, axial deflections, and lateral deflections at strategic locations on each wall. The deformations were measured from zero load to failure in 10 kip (4530 kgf) increments. In addition, concrete cylinder strengths and ultimate loads were obtained for each wall.

The test walls were modeled to conform with the requirements of the ACI Building Code, and were used to predict the structural behavior and ultimate strength of full-scale walls currently used in engineering practice. The research program involved the use of the experimental results to attempt to verify the analytical methods used in design practice at this time, and to make recommendations for modification of the design practice, if advisable.

Every attempt was made to develop pinned-end conditions at the top and bottom of the walls.

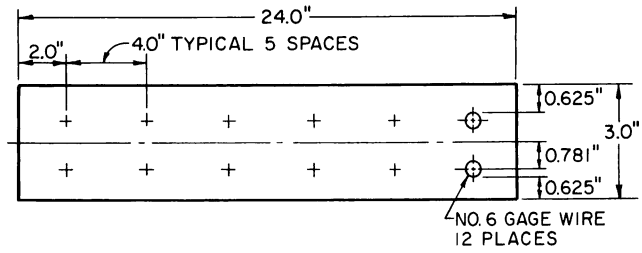

(a) NO. 6 GAGE WIRE WITH 5/8" COVER.

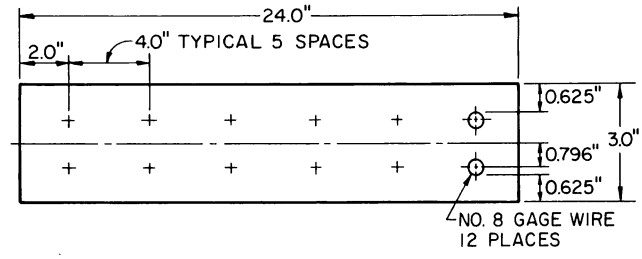

(b) NO. 8 GAGE WIRE WITH 5/8" COVER

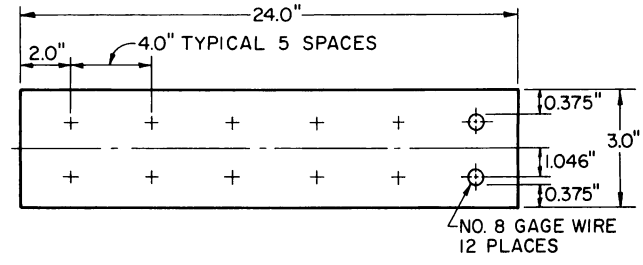

(c) NO. 8 GAGE WIRE WITH 3/8" COVER

Fig. 1—Location of steel reinforcement

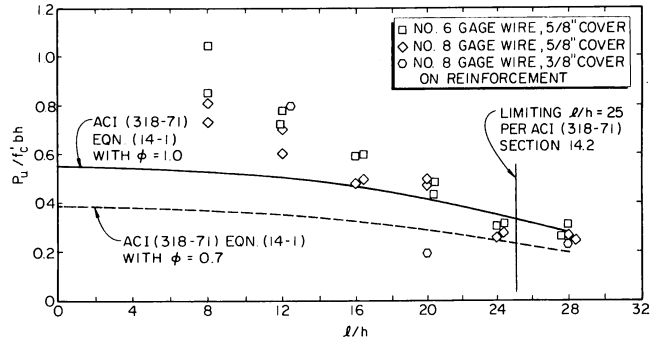

Fig. 2—Comparison of ultimate failure loads of test walls with an eccentric load with the ACI Building Code Eq. (14-1) for the design of walls

Loads were applied through a bearing system which permitted the wall ends to rotate.

ANALYSIS BY THE ACI BUILDING CODE EMPIRICAL EQUATION

Fig. 2 shows dimensionless quantities of failure loads and height-to-thickness ratios for all eccentrically loaded walls ($e/h = 1/6$) in the test program. Fig. 3 shows dimensionless quantities of failure loads and height-to-thickness ratios for all concentrically loaded walls ($e/h = 0$) in the program. The solid curve in Fig. 2 and 3 shows the

TABLE 1—WALL PANEL DESIGNATIONS AND CYLINDER STRENGTHS

Wall panel designation	Date cast	Date of test	Curing time, days	Cylinder failure load, kips	Cylinder compressive strength, psi	Average cylinder strength for each wall height, psi	Coefficient of variation, percent
A-2-2-P	4/11/72	8/4/72	115	87.5	3094		
B-2-2-P	4/11/72	8/4/72	115	107.5	3801		
A-2-1-P	4/8/72	8/5/72	119	91.5	3251		
B-2-1-P	4/8/72	8/5/72	119	69.5	2458	3814	26.34
A-2-2-M	4/13/72	8/7/72	116	144.5	5110		
B-2-2-M	4/13/72	8/7/72	116	131.0	4632		
A-2-1-M	4/13/72	8/9/72	118	111.0	3925		
B-2-1-M	4/13/72	8/9/72	118	120.0	4243		
A-3-1-MC	5/8/72	8/11/72	95	105.0	3713		
B-3-1-MC	5/8/72	8/11/72	95	122.5	4332		
A-3-2-P	5/4/72	8/12/72	98	106.5	3776		
B-3-2-P	5/4/72	8/12/72	98	107.0	3784	3737	8.85
A-3-1-P	5/2/72	8/13/72	102	115.5	4084		
B-3-1-P	5/2/72	8/13/72	103	85.5	3023		
A-3-2-M	5/5/72	8/14/72	101	105.5	3731		
B-3-2-M	5/5/72	8/14/72	101	98.0	3465		
A-3-1-M	5/4/72	8/14/72	102	102.0	3607		
B-3-1-M	5/4/72	8/14/72	102	109.3	3865		
A-4-2-P	5/11/72	8/23/72	106	164.0	5799		
B-4-2-P	5/11/72	8/23/72	106	143.5	5074		
A-4-1-P	5/10/72	8/25/72	109	132.5	4685		
B-4-1-P	5/10/72	8/26/72	110	141.5	5003	5010	10.30
A-4-2-M	5/13/72	8/26/72	107	142.5	5039		
B-4-2-M	5/13/72	8/26/72	107	137.0	4844		
A-4-1-M	5/11/72	8/28/72	111	113.5	4013		
B-4-1-M	5/11/72	8/28/72	111	159.0	5622		
A-5-1-MC	4/25/72	7/28/72	94	63.5	2245		
B-5-1-MC	4/25/72	8/1/72	98	55.0	1945		
A-5-2-P	5/17/72	12/28/72	225	164.5	5817		
B-5-2-P	5/17/72	12/29/72	226	173.0	6117	5621	4.24
A-5-1-P	5/16/72	12/29/72	227	147.3	5209		
B-5-1-P	5/16/72	12/29/72	227	176.5	6241		
A-5-2-M	5/18/72	9/4/72	109	165.5	5852		
B-5-2-M	5/18/72	9/9/72	114	154.5	5463		
A-5-1-M	5/17/72	8/19/72	94	168.5	5958		
B-5-1-M	5/17/72	8/17/72	92	122.0	4314		
A-6-2-P	5/24/72	1/3/73	223	186.0	6577		
B-6-2-P	5/24/72	1/3/73	223	160.0	5658		
A-6-1-P	5/22/72	1/4/73	226	196.0	6931		
B-6-1-P	5/22/72	1/5/73	227	208.0	7355	6674	7.23
A-6-2-M	5/24/72	1/5/73	225	195.5	6913		
B-6-2-M	5/24/72	1/5/73	225	180.5	6383		
A-6-1-M	5/23/72	1/5/73	226	185.0	6542		
B-6-1-M	5/23/72	1/5/73	226	199.0	7036		
A-7-1-MC	5/23/72	1/9/73	230	179.0	6330		
B-7-1-MC	5/23/72	1/9/73	227	170.5	6028		
A-7-2-P	6/13/72	1/15/73	216	152.5	5393		
B-7-2-P	6/13/72	1/15/73	216	162.5	5747	5981	5.03
A-7-1-P	6/8/72	1/16/73	222	185.0	6542		
B-7-1-P	6/8/72	1/17/73	223	153.0	5410		
A-7-2-M	6/15/72	1/18/73	217	173.0	6117		
B-7-2-M	6/15/72	1/19/73	218	186.5	6595		
A-7-1-M	6/9/72	1/19/73	224	155.5	5499		
B-7-1-M	6/9/72	1/19/73	224	174.0	6152		

1 kip = 453.6 kgf; 1 psi = 0.07031 kgf/cm^2

ACI Building Code Eq. (14-1), stated in Section 14.2, for empirical design of walls without the understrength factor $\phi = 0.7$ applied.

Fig. 2 shows ultimate loads are well above the values obtained using the empirical equation for small height-to-thickness ratios, 8 through 12. However, for height-to-thickness ratios of 16 through 20, values obtained from the equation coincide with test data. Walls beginning at values of l/h equal to 16 exhibited buckling failures for eccentric loads. Walls with height-to-thickness ratios of 24 through 28 show failure loads below the equation values, without the ϕ factor applied. The height-to-thickness ratio of 24 falls within the limits of the ACI Building Code relative to the empirical equation, whereas the value of 28 exceeds the maximum value of 25 given in Chapter 14 of the code.

The one low value of failure load in the $l/h = 20$ group is Panel B-5-1-MC. This is due to the shorter curing time and concrete cylinder strength of this particular test wall compared to the other walls in the $l/h = 20$ group, reference Table 1. The wall strength curve of Fig. 2 is based on average concrete strength for each wall height. Values of $P_u/f_c'bh$ are also based upon average values of f_c' for each wall height.

Fig. 4 shows $P_u/f_c'bh$ values based upon the concrete cylinder strength for each wall. This presentation of data shows the Panel B-5-1-MC failure load to correspond more closely with the other values in the $l/h = 20$ wall group.

TABLE 2—WALL PANEL DESIGNATIONS AND LOAD CONDITIONS

Wall height, ft	Wall panel designation	Reinforcement size (wire number)	Reinforcement cover, in.	Load condition	Wall width, ft	Wall thickness, in.
2	A-2-2-P	#6 gage	5/8	concentric	2	3
2	B-2-2-P	#6 gage	5/8	concentric	2	3
2	A-2-1-P	#8 gage	5/8	concentric	2	3
2	B-2-1-P	#8 gage	5/8	concentric	2	3
2	A-2-2-M	#6 gage	5/8	eccentric	2	3
2	B-2-2-M	#6 gage	5/8	eccentric	2	3
2	A-2-1-M	#8 gage	5/8	eccentric	2	3
2	B-2-1-M	#8 gage	5/8	eccentric	2	3
3	A-3-1-MC	#8 gage	3/8	concentric	2	3
3	B-3-1-MC	#8 gage	3/8	eccentric	2	3
3	A-3-2-P	#6 gage	5/8	concentric	2	3
3	B-3-2-P	#6 gage	5/8	concentric	2	3
3	A-3-1-P	#8 gage	5/8	concentric	2	3
3	B-3-1-P	#8 gage	5/8	concentric	2	3
3	A-3-2-M	#6 gage	5/8	eccentric	2	3
3	B-3-2-M	#6 gage	5/8	eccentric	2	3
3	A-3-1-M	#8 gage	5/8	eccentric	2	3
3	B-3-1-M	#8 gage	5/8	eccentric	2	3
4	A-4-2-P	#6 gage	5/8	concentric	2	3
4	B-4-2-P	#6 gage	5/8	concentric	2	3
4	A-4-1-P	#8 gage	5/8	concentric	2	3
4	B-4-1-P	#8 gage	5/8	concentric	2	3
4	A-4-2-M	#6 gage	5/8	eccentric	2	3
4	B-4-2-M	#6 gage	5/8	eccentric	2	3
4	A-4-1-M	#8 gage	5/8	eccentric	2	3
4	B-4-1-M	#8 gage	5/8	eccentric	2	3
5	A-5-1-MC	#8 gage	3/8	concentric	2	3
5	B-5-1-MC	#8 gage	3/8	eccentric	2	3
5	A-5-2-P	#6 gage	5/8	concentric	2	3
5	B-5-2-P	#6 gage	5/8	concentric	2	3
5	A-5-1-P	#8 gage	5/8	concentric	2	3
5	B-5-1-P	#8 gage	5/8	concentric	2	3
5	A-5-2-M	#6 gage	5/8	eccentric	2	3
5	B-5-2-M	#6 gage	5/8	eccentric	2	3
5	A-5-1-M	#8 gage	5/8	eccentric	2	3
5	B-5-1-M	#8 gage	5/8	eccentric	2	3
6	A-6-2-P	#6 gage	5/8	concentric	2	3
6	B-6-2-P	#6 gage	5/8	concentric	2	3
6	A-6-1-P	#8 gage	5/8	concentric	2	3
6	B-6-1-P	#8 gage	5/8	concentric	2	3
6	A-6-2-M	#6 gage	5/8	eccentric	2	3
6	B-6-2-M	#6 gage	5/8	eccentric	2	3
6	A-6-1-M	#8 gage	5/8	eccentric	2	3
6	B-6-1-M	#8 gage	5/8	eccentric	2	3
7	A-7-1-MC	#8 gage	3/8	concentric	2	3
7	B-7-1-MC	#8 gage	3/8	eccentric	2	3
7	A-7-2-P	#6 gage	5/8	concentric	2	3
7	B-7-2-P	#6 gage	5/8	concentric	2	3
7	A-7-1-P	#8 gage	5/8	concentric	2	3
7	B-7-1-P	#8 gage	5/8	concentric	2	3
7	A-7-2-M	#6 gage	5/8	eccentric	2	3
7	B-7-2-M	#6 gage	5/8	eccentric	2	3
7	A-7-1-M	#8 gage	5/8	eccentric	2	3
7	B-7-1-M	#8 gage	5/8	eccentric	2	3

1 in. = 2.54 cm; 1 ft = 30.48 cm; #6 gage is approx. 0.5 cm; #8 gage is approx. 0.4 cm.

When the ϕ factor is applied to the equation, the equation plots below all test loads but shows marginal results for large height-to-thickness ratios. Two items are worth noting in comparing these test loads with the ACI Building Code equation values. First, walls in the test program had ratios of area of steel to concrete of 0.0033 and 0.0047. These values are considerably higher than the 0.0015 minimum ratio specified by Chapter 14 of the ACI Building Code. Therefore, had smaller ratios been incorporated in the testing program, failures could be expected to be below the ACI Building Code equation values for large height-to-thickness ratios, even with the ϕ factor applied. Second, pinned-end conditions were used for all test wall panels. In current industry practice, a pinned-end condition is not only difficult to create

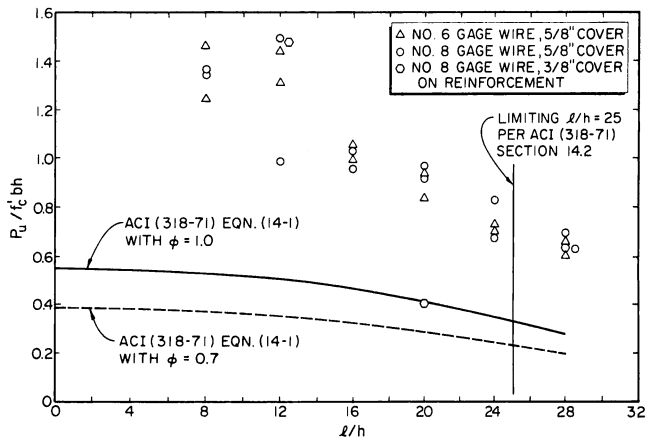

Fig. 3—Comparison of ultimate failure loads of test walls with a concentric load with the ACI Building Code Eq. (14-1) for the design of walls

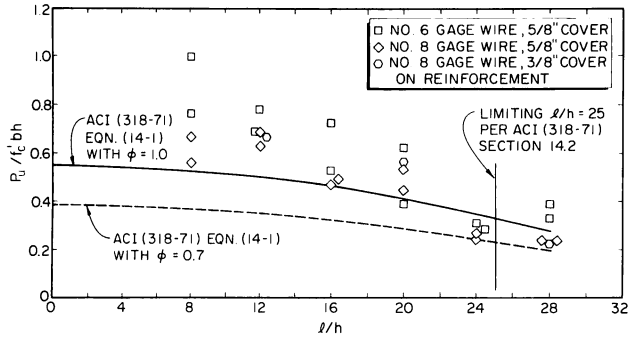

Fig. 4—Comparison of ultimate failure loads of test walls with an eccentric load with the ACI Building Code Eq. (14-1) for the design of walls

but also unrealistic. Actual end conditions closely approach fixity. However, no end condition requirements are imposed by the ACI Building Code for wall design by the empirical Eq. (14-1) and pinned-ends are normally assumed; therefore, the comparison of failure loads of the test program with the equation is appropriate. Also, the effect of end conditions influences wall strength by the term $(kl)^2$. Any fixity of the ends of the wall would increase failure loads above those obtained from the pinned-end condition used in the test program.

ANALYSIS ASSUMING THE WALLS TO ACT AS COLUMNS

Interaction diagrams were developed for the three wall configurations in the test program, considering the walls to act as columns. The values used in plotting the curves were obtained from the Portland Cement Association computer program for ultimate strength design of reinforced concrete columns.[3] Execution of the program was performed at The University of Texas at Arlington. All limits of the ACI Building Code are incorporated into the computer program. The wall configurations of the test program were defined as tied columns to obtain the interaction curves.

Development of interaction curves provides ultimate capacity of the members for combinations of axial load and moment at various eccentricities of load. However, the effects of slenderness are not incorporated into the curves. Since wall sections generally maintain large heights in comparison to their thickness, the effects of slenderness must be included to accurately determine the behavior of the member.

Chapter 10 of the ACI Building Code contains provisions for slenderness effects of members subjected to flexure and axial load. Section 10.11.5 of the code considers the effect of slenderness by a magnified moment in Eq. (10-4).

Fig. 5 shows ultimate strength analysis by Chapter 10 of the ACI Building Code for walls with an eccentric load ($e/h = 1/6$), without the understrength factor ϕ applied. Failure loads are based on average cylinder strength for each wall height. Interaction diagram values of $P_u/(f_c'bh)$ for each kl/h showed no distinguishable difference for the different sizes of reinforcement used in the test program. The solid curve of Fig. 5 assumes that the predicted strength of the three wall configurations will be identical for any particular value of kl/h.

The dashed line in the kl/h range of 0 to 8 represents analytical computations for the maximum and minimum values of concrete strength in the test program. This is shown to provide a complete theoretical column analysis for the test program, although no test walls were built in this range of height-to-thickness ratios.

As previously discussed the one low failure load in the $l/h = 20$ group of Fig. 5 in Panel B-5-1-MC and is due to the lower concrete strength of this wall compared to other panels in this wall height. Fig. 6 shows failure loads based upon concrete

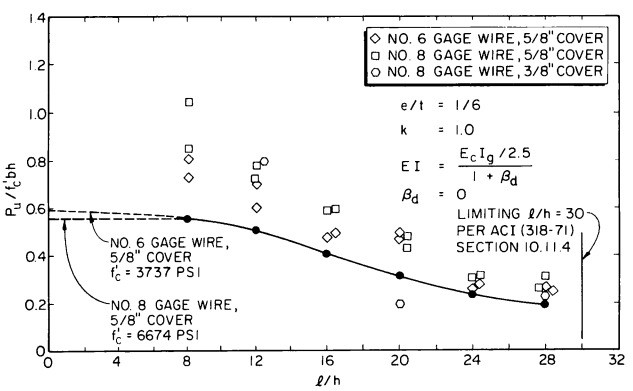

Fig. 5—Comparison of ultimate failure loads of test walls with an eccentric load ($e/h = 1/6$) to the magnified moment design procedure of Chapter 10 of the ACI Building Code

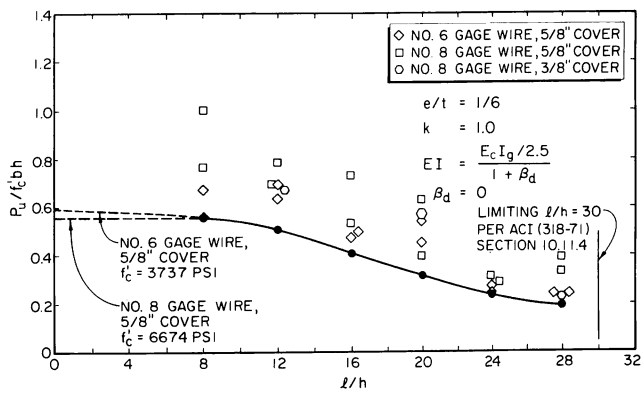

Fig. 6—Comparison of ultimate failure loads of test walls with an eccentric load ($e/h = 1/6$) to the magnified moment design procedure of Chapter 10 of the ACI Building Code

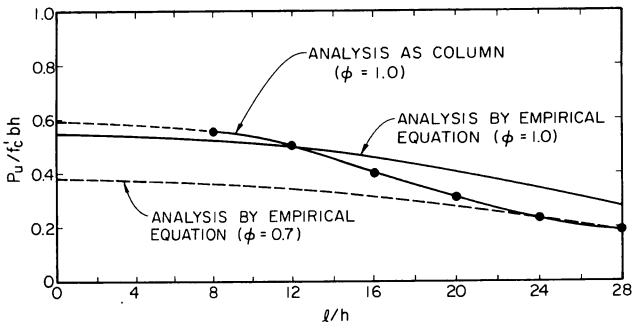

Fig. 7—Comparison of empirical equation for wall design to analysis of a wall as a column

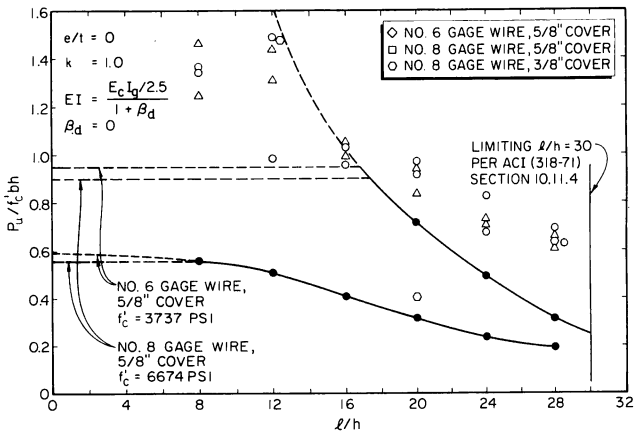

Fig. 8—Comparison of ultimate failure of test walls with a concentric load ($e/h = 0$) to the Euler buckling (upper curve) and Chapter 10 (lower curve) of the ACI Building Code

cylinder strength for each wall which shows the Panel B-5-1-MC failure load to correspond more closely with the other values in the $l/h = 20$ wall group.

Column analysis predicts ultimate loads well below the actual failure loads for small and intermediate height-to-thickness ratios (8 through 20). Large height-to-thickness ratio analysis (ratios 24 and 28) show a close correlation between the theoretical loads and failure loads of the test walls. The effect of end restraints is more sensitive to large wall heights since the strength of the wall is influenced by the term $(kl/h)^2$. Chapter 10 of the ACI Building Code allows height-to-thickness ratios of 30, which is above the maximum value of 28 used for the test walls and the maximum value of 25 in Chapter 14 of the code for wall design.

Fig. 7 shows a comparison of analytical results obtained using the empirical equation and the analytical method stated in Chapter 10 of the ACI Building Code, which permits walls to be designed as columns. The steel strength and location in the wall used in this analysis is based upon those used in the test walls. It is important to note that the empirical equation predicts higher strength (for $\phi = 1$) than that predicted by the column design method for l/h greater than 12.

The ACI Building Code recognizes the inherent possibility of induced eccentricities caused by numerous factors: initial curvature of the member, dislocated reinforcement, etc. Therefore Chapter 10 of the code requires design of compression members for a minimum eccentricity of $e/h = 1/10$ or $e = 1$ in. (2.54 cm), whichever is greater.

Concentrically loaded walls are shown in Fig. 8 with two methods of predicted load. The upper predicted ultimate strength curve is based upon the Euler buckling load $P_u = \pi^2 EI/l^2$ with $EI = E_c I_g/2.5(1 + \beta_d)$. The horizontal dashed lines intersecting this curve represents limiting values of failure loads based upon concrete strength. The lower predicted strength curve is based upon the ACI Building Code requirement to design for a minimum eccentricity of $e/h = 1/10$ or $e = 1$ in. (2.54 cm), whichever is greater. Since walls were considered half scale models, an $e = \frac{1}{2}$ in. would produce an $e/h = 1/6$. Since this value is larger than $e/h = 1/10$, the lower curve of Fig. 8 is based on an $e/h = 1/6$.

SUMMARY OF TEST RESULTS

1. Bearing stress failures occurred at the end surfaces where load was applied for 2 ft (60.96 cm) high walls ($l/h = 8$). Therefore, this height-to-thickness ratio can be classified as representing short column action.

2. Three ft (91.44 cm) high concentrically loaded walls ($l/h = 12$) showed a scatter in locations of failures. Two failed at the end surfaces and two at the center of the wall. Eccentrically loaded walls all failed at the end surfaces.

3. Concentrically loaded 4 ft (121.92 cm) high walls ($l/h = 16$) exhibited randomness in locations of failures. Also, numerous horizontal cracks developed at several locations on the wall. Walls with l/h equal to and greater than 16 buckled under eccentric load and collapsed at failure.

4. Five ft (152.40 cm) high concentrically loaded walls ($l/h = 20$) all showed failures to occur horizontally at the center line. Eccentrically loaded walls exhibited buckling failures.

5. Center line failures occurred for all 6 ft (182.88 cm) high ($l/h = 24$) concentrically loaded walls. Eccentrically loaded walls failed by buckling similar to 4 and 5 ft (121.92 and 152.40 cm) high walls which had l/h of 16 and 20.

6. Seven ft (213.36 cm) high walls ($l/h = 28$) with a concentric load failed by buckling similar

to walls with l/h from 16 through 24 with an eccentric load. Due to a reduced rate of loading, most 7 ft (213.36 cm) high walls with an eccentric load did not buckle from the testing machine but developed numerous horizontal cracks which extended from the tension face through the wall thickness to within approximately ¼ in. (0.635 cm) from the compression face.

7. For concentrically loaded walls, eight deflected in the forward direction, eighteen deflected in the backward direction, and one deflected in double curvature.

8. For small height-to-thickness ratios (8 through 20), walls with a concentric load had lateral deflections that did not increase at the instant of failure. This includes the 2 through 5 ft (60.96 through 152.40 cm) high walls.

9. For 6 and 7 ft (182.88 and 213.36 cm) high walls ($l/h = 24$ and 28) with a concentric load, the lateral deflections at failure were undefined and continually increased at the instant of failure and could not be read from the dial gages.

10. For 2 through 4 ft (60.96 through 121.92 cm) high walls ($l/h = 8$ through 16), walls with an eccentric load had lateral deflections that did not increase at the instant of failure and could be read from the dial gages.

11. For height-to-thickness ratios of 20 and larger, lateral deflections of eccentrically loaded walls were undefined at failure, and continually increased at the instant of failure and could not be read from the dial gages.

12. Walls with l/h of 8 and 12 showed a linear relationship between concentric load and strain for loads from zero to approximately 80 percent of ultimate load. For l/h of 16 and 20 the linear relation shows to be approximately 70 percent and reduces to approximately 60 percent for l/h of 24 and 28.

13. For l/h of 8 and 12, walls with an eccentric load showed a linear relationship between load and strain from zero to approximately 30 percent of ultimate load. Values of l/h from 16 through 28 showed a nonlinear relationship between load and strain from approximately zero load to ultimate load.

14. Surface strains were quite sensitive to the time-dependent behavior of concrete.

CONCLUSIONS

Each wall was analyzed in accordance with the ACI Building Code (ACI 318-71). Analysis of the code's empirical equation for wall design predicts ultimate loads considerably lower than failure loads for small l/h values (8 to 12). For intermediate height-to-thickness ratios (16 to 20), results predicted by the equation are compatible with failure loads. For large height-to-thickness ratios (24 to 28), test failure loads are below the loads predicted by the equation. Any fixity of the end restraints of the test walls would increase failure loads above the values obtained from the test program. However, in design practice, pinned-ends are normally assumed. Thus, the use of pinned-ends in this research was considered to be appropriate. Test loads plotted above the equation values when the understrength factor $\phi = 0.7$ was applied.

The following equation has been developed by the authors which predicts the ultimate failure loads of reinforced concrete wall panels:

$$P_u = 0.60\phi f_c' bh\,[1 - (l/30h)^2] \qquad (1)$$

This equation has been derived based upon test results of the 54 wall panels tested in the investigation. Fig. 9 shows the predicted strength of walls by this equation compared with the values of $P_u/f_c'bh$ (based upon average cylinder strengths for each wall height) for all walls with an eccentric load tested in the investigation. Fig. 10 shows the predicted strength by this equation compared with values of $P_u/f_c'bh$ (based upon concrete

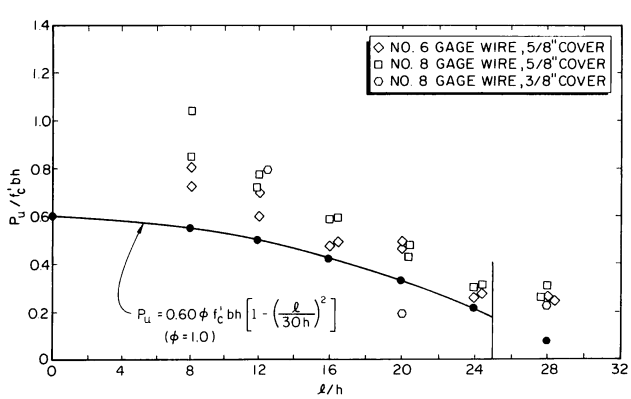

Fig. 9—Comparisons of proposed equation for two layers of reinforcement with ultimate failure loads of test walls with an eccentric load

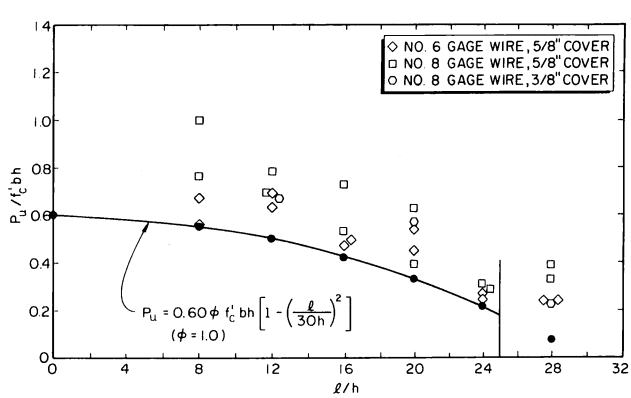

Fig. 10—Comparisons of proposed equation for two layers of reinforcement with ultimate failure loads of test walls with an eccentric load

cylinder strength for each wall) for all walls with an eccentric load tested in the investigation. All failure loads show higher than predicted with the understrength factor $\phi = 1.0$.

It should be noted that all walls tested in the investigation had two layers of reinforcement. Thus the above equation can be used to predict ultimate failure loads only for walls with two rows of reinforcement. Additional tests should be conducted to determine the ultimate failure load for walls with a single layer of reinforcement.

Fig. 11 shows a comparison of the equation with the analysis methods of Chapters 10 and 14 of the ACI Building Code.

Each wall was also analyzed as a rectangular column by ultimate strength methods in accordance with Chapter 10 of the ACI Building Code. This method of analysis proves to be very compatible and frequently conservative when compared with failure loads through the entire range of height-to-thickness ratios used in the testing program. Analysis shows marginal results for larger height-to-thickness ratios; however, any degree of end restraint other than the pinned-end condition used in the test program would have increased the test failure loads. This is particularly true of large wall heights since the strength is influenced by the term $(kl)^2$. That method of analysis also proved to be valid for concentrically loaded walls.

Therefore, the ultimate strength analysis as columns, including slenderness effects, correlates well with test data and is recommended as the proper method for designing wall panels. However, the method is somewhat conservative for small l/h values (8 and 12). This procedure accounts for reinforcement location, tensile strength, and all variables including slenderness effects. The empirical equation method of Chapter 14 of the ACI Building Code has been shown to be valid for l/h values up to 20. For l/h values larger than 20, the method predicts loads below test failure loads only when the $\phi = 0.7$ factor is applied.

Using the configuration of steel location and the size and strength of steel utilized in the research program, the column design method predicts considerably less strength than does the empirical method for l/h values larger than 12.

In general, the method of Chapter 10 of the ACI Building Code is superior to the empirical method of Chapter 14. However, Chapter 10 of the code cannot be applied for designing walls without using certain provisions of Chapter 14. It would seem to be appropriate to move all design provisions for walls to Chapter 14, to correlate the two methods for wall design and to state the limitations for the empirical method.

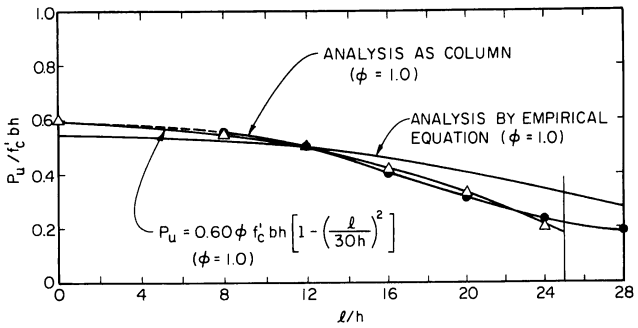

Fig. 11—Comparison of empirical equation of Chapter 14 of the ACI Building Code, the proposed equation, and the analysis of walls as a column

In current design practice, tilt-up walls have been constructed, and have served satisfactorily, despite the fact that they do not conform with the provisions of the ACI Building Code. In particular, kl/h values have been used up to 150, with base supports consisting of simple slots or dowels into grade beams, and upper-end lateral supports consisting only of the top chords of bar joists; yet, no failures of such walls have been reported.

Since the tilt-up method of construction of wall panels is growing in popularity, it is essential that ACI provide a means of controlling this method of construction.

REFERENCES

1. ACI Committee 318, "Building Code Requirements for Reinforced Concrete (ACI 318-71)," American Concrete Institute, Detroit, 1971, 78 pp. (plus cumulative supplement issued annually).
2. Oberlender, Garold D., "Strength Investigation of Precast Reinforced Concrete Load Bearing Wall Panels," PhD Dissertation, University of Texas, Arlington, 1973.
3. "IBM 1130 Computer Program for the Ultimate Strength Design of Reinforced Concrete Columns," Portland Cement Association, 1967.
4. Kerekes, Frank, and Reid, Harold B., "Fifty Years of Development in Building Code Requirements for Reinforced Concrete," ACI JOURNAL, *Proceedings* V. 50, No. 6, Feb. 1954, pp. 441-470.
5. ACI Committee 533, "Design of Precast Concrete Wall Panels," ACI JOURNAL, *Proceedings* V. 68, No. 7, July 1971, pp. 504-513.
6. Smith, J. D., and Sidebottom, O. M., *Elementary Mechanics of Deformable Bodies*, The MacMillan Co., London, 1969, p. 63.
7. ACI Committee 214, "Recommended Practice for Evaluation of Compression Test Results of Field Concrete (ACI 214-65)," American Concrete Institute, Detroit, 1965, 28 pp.
8. Whitney, Charles S., "Plastic Theory of Reinforced Concrete Design," *Transactions*, ASCE, V. 107, 1942, pp. 251-282.
9. Everard, Noel J., and Cohen, Edward, *Ultimate Strength Design of Reinforced Concrete Columns*, SP-7, American Concrete Institute, Detroit, 1964, 182 pp.

Received Sept. 15, 1975, and reviewed under Institute publication policies.